Polyhedron 30 (2011) 1149–1156

Contents lists available at ScienceDirect

Polyhedron

journal homepage: www.elsevier.com/locate/poly

Coordination properties of axially unfixed chiral dipyridine ligands towards metal and ammonium ions

Kiu-Chor Sham [a], Chi-Sing Lee [a,b], Ka-Yee Chan [a], Shek-Man Yiu [a], Wing-Tak Wong [c], Hoi-Lun Kwong [a,*]

[a] Department of Biology and Chemistry, City University of Hong Kong, 83 Tat Chee Avenue, Kowloon Tong, Hong Kong Special Administrative Region
[b] Laboratory of Chemical Genomics, Shenzhen Graduate School of Peking University, Shenzhen University Town, Xili, Shenzhen, China
[c] Department of Chemistry, The University of Hong Kong, Pokfulam Road, Hong Kong Special Administrative Region

ARTICLE INFO

Article history:
Received 14 October 2010
Accepted 13 January 2011
Available online 3 February 2011

Dedicated to Professor K. Barry Sharpless for the occasion of his 70th birthday

Keywords:
Chiral ligand
Dipyridine ligand
Metal binding
Ammonium ions binding
Copper complex
Silver complex

ABSTRACT

New chiral dipyridine ligands with an axially unfixed 1,1′-biphenyl bridge were prepared via homocoupling of bromophenyl pyridines. The conformeric ratios of the free ligands in solution and their coordination properties towards metal ions were studied by NMR spectroscopy. X-Ray crystallography of the silver(I) and copper(I) complexes showed 1:1 metal to ligand complexes and *S* planar chirality. Interestingly, the biphenyl ligands show a 1:2 stepwise binding towards most ammonium ions tested with strong fluorescence enhancement, but a selectively 1:1 binding towards L-ornithine methyl ester hydrochloride with no fluorescence enhancement.

1. Introduction

Pyridine is one of the best known ligands in coordination chemistry. By choosing a suitable linker to connect two units together, a bidentate ligand can be constructed [1]. The linker is very important in the coordination chemistry of this ligand because it affects its important properties, such as binding angle, donating property and coordination geometry [2–8]. The 1,1′-biphenyl bridge is one of the linkers used in ligand design. A number of polydentate ligands have been developed based on this linker and their coordination properties towards various metal ions have been extensively studied [9–19].

With the biphenyl bridge, the two aromatic rings can rotate around an axially unfixed bridge through the C–C single bond, which could allow the ligand to act as a bridging ligand for binding two different cations. For example, Stein and coworkers recently reported a mixed valence diiron complex with a biphenyl-bridged dithiolate as the bridging ligand [20]. The interesting optical and electronic properties associated with the inter-ring twisting angles between the two phenyl rings [21] make ligands with a 1,1′-biphenyl bridge potential sensors [22–28]. We have been interested in developing new chiral pyridine-containing ligands for asymmetric catalysis and molecular recognition [29]. To extend the scope of our study, we decided to incorporate a 1,1′-biphenyl bridge into a bipyridine ligand. Herein, we report the synthesis of the new biphenyl ligands **L1** and **L2** and their interesting coordination properties towards metal and ammonium ions.

2. Synthesis of the biphenyl ligands (L1 and L2)

The biphenyl ligands **L1** and **L2** were readily prepared from 2′-bromoacteophone via a three-step sequence with 30–37% overall isolated yields. As shown in Scheme 1 2′-bromoacteophone was converted to pyridinium iodide **1** using iodine in pyridine at 90 °C. A subsequent Kröhnke condensation of **1** with chiral ketones **2**–**3** gave the bromophenyl pyridine intermediates **4**–**5** in 42–58% yields [30]. Finally, an Ullmann coupling of the bromophenyl pyridines **4**–**5** using copper powder in 100 °C degassed DMF afforded the expected biphenyl ligands **L1**–**2** in 46–80% yields, which were characterized unambiguously by ^{1}H and ^{13}C NMR, ESI-MS and elemental analysis.

3. Conformational analysis using NMR studies

The ^{1}H NMR spectra of **L1** and **L2** in deuterated chloroform showed two sets of signals, indicating the presence of two conformers in solution. These two conformers could be caused by a

* Corresponding author.
E-mail address: bhhoik@cityu.edu.hk (H.-L. Kwong).

0277-5387/$ - see front matter © 2011 Elsevier Ltd. All rights reserved.
doi:10.1016/j.poly.2011.01.017

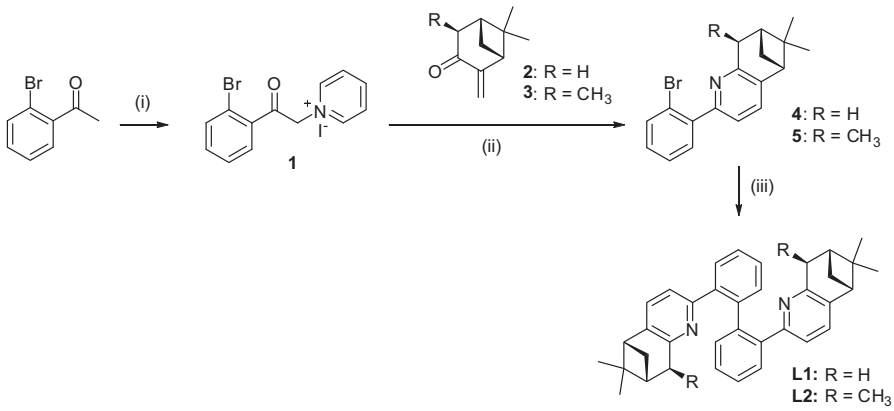

Scheme 1. Synthesis of the biphenyl ligands **L1** and **L2**. Reaction conditions: (i) I_2, pyridine, 90 °C; (ii) ammonium acetate, acetic acid, 110 °C; (iii) Cu, degassed DMF, 100 °C.

slow rotation around the C–C single bond of the biphenyl backbone (Fig. 1). The ratios of the two rotational conformers were determined by comparing a pair of well resolved signals (H_A and $H_{A'}$) in the aromatic region (Fig. 2). The conformeric ratios of the biphenyl ligands were then studied in different NMR solvents. As shown in Table 1, **L2** shows only a slightly higher conformeric ratio than **L1** (entries 1 and 5), suggesting the two chiral pyridines of the free ligands are not closed enough to induce the formation of the major conformer. Other aprotic solvents, including acetone-d_6 and benzene-d_6, also give a roughly 1:1 ratio of conformers (entries 2, 3 and 6). Interestingly, methanol-d_4 gives a significantly higher conformeric ratio (70:30), which indicates hydrogen bonding formation between the pyridine rings of the ligands and the solvent molecules (entries 4 and 7). By determining the NMR coalescence temperature, **L2** has an activation barrier of 13.6 kcal/mol to axial torsion and an interconversion rate of 32 s^{-1} between the two conformers at 50 °C [31].

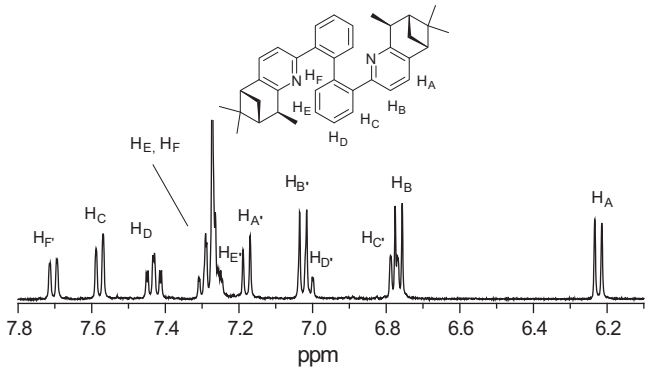

Fig. 2. The aromatic region of the ^1H NMR spectrum of **L2** (H_A = major isomer; $H_{A'}$ = minor isomer) in $CDCl_3$.

4. Coordination properties towards metal ions

After the conformational analysis of the free ligands in solution, the effects of metal–ligand interactions on the equilibration between the two rotational conformers were studied using NMR titration experiments. Upon addition of $AgClO_4$, the two sets of NMR signals collapsed slowly as a new set of signals appeared (Fig. 3). The ratio of the conformers did not change during the titration and no further change was observed with more than one equivalent of $AgClO_4$. The silver(I) complexes of **L1** and **L2** can be directly synthesized by stirring the ligand with $AgClO_4$ in methanol. The ESI-MS spectra of the complexes gave signals that corresponding to the single charged species $[Ag(\mathbf{L})]^+$ at 603 and 631, suggesting formation of the mononuclear complexes. The empirical formula of the silver(I) complexes $[Ag(\mathbf{L})ClO_4]$ was further confirmed by elemental analysis. The ^1H NMR spectrum of $[Ag(\mathbf{L2})ClO_4]$ showed a single diastereomer in $CDCl_3$, which is consistent with the results of the previous NMR titration experiments. However, a 4:1 diastereomeric ratio (60% de) was observed in the ^1H NMR spectrum of $[Ag(\mathbf{L1})ClO_4]$ (Fig. 4).

The copper(I) complexes of **L1** and **L2** were also prepared by a similar procedure with CuI in degassed acetonitrile. The biphenyl ligands showed similar coordination properties towards both silver(I) and copper(I) ions, and they also formed a 1:1 metal–ligand

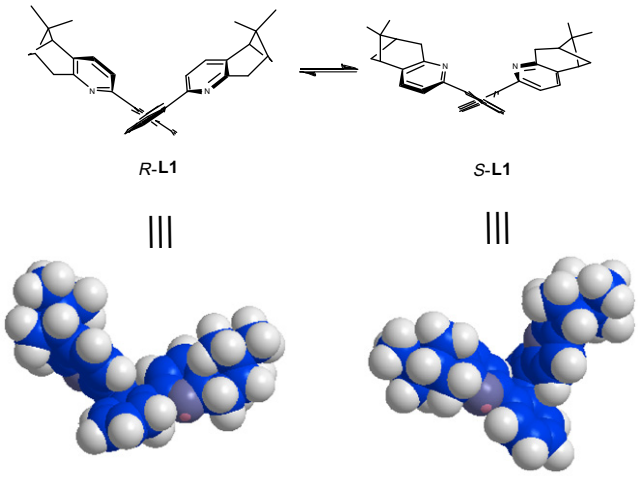

Fig. 1. Equilibration between the two rotational conformers of **L1**. The space filling models were generated using Chem3D.

Table 1
The ratio of biphenyl conformers in different NMR solvents.

Entry	Ligand	Solvent	Conformer ratio[a,b]
1	**L1**	Chloroform-*d*	55:45
2		Acetone-d_6	56:44
3		Benzene-d_6	53:47
4		Methanl-d_4	70:30
5	**L2**	Chloroform-*d*	59:41
6		Benzene-d_6	51:49
7		Methanl-d_4	70:30

[a] The ratio of the rotational conformers was determined by comparing a pair of well resolved signals in either ^1H or ^{13}C NMR spectra.
[b] Determined at 18.7 °C.

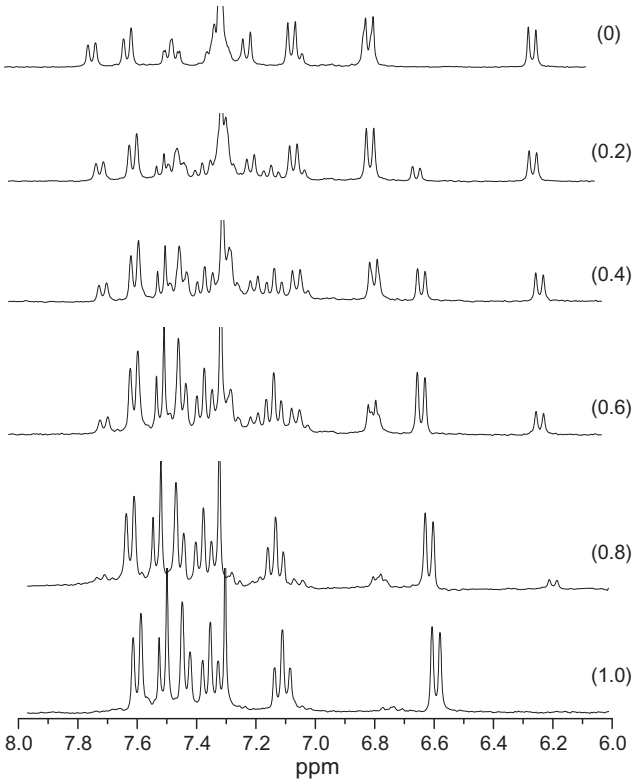

Fig. 3. ^{1}H NMR titration study of **L2** towards $AgClO_4$ in $CDCl_3$, [**L2**] = 0.014 M and $AgClO_4$ = 0 to 0.014 M. The numbers in parentheses indicated the number of equivalents of $AgClO_4$ added.

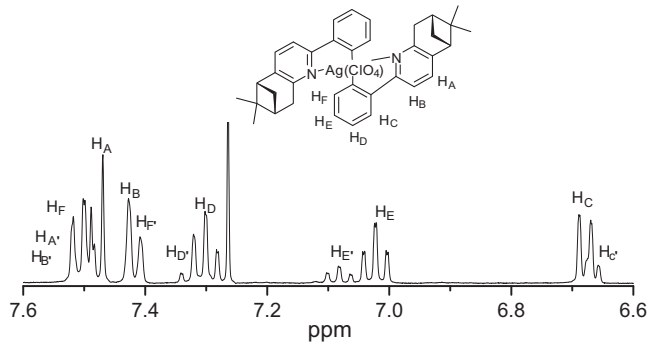

Fig. 4. The aromatic region of the ^{1}H NMR spectrum of [Ag(**L1**)ClO_4] (H_A = major isomer; $H_{A'}$ = minor isomer) in $CDCl_3$. The drawing shows the major isomer.

complex with the copper(I) ion. The copper(I) complex of **L2** was found to be a single diastereomer and a 2.9:1 diastereomeric ratio (49% de) was obtained for the copper(I) complex of **L1**.

5. Crystal structures of the silver(I) and copper(I) complexes

Single crystals of [Ag(**L2**)ClO_4] and [Cu(**L2**)I] were obtained by slow diffusion methods. The ORTEP plots and space-filling diagrams of the crystal structures are shown in Figs. 5 and 6. Both crystal structures show *S* planar charity which suggests that they should be the major diastereomers observed in solution. As showed in Fig. 5, the silver(I) ion has a distorted tetrahedral geometry, coordinating to the two pyridines of **L2** and two oxygens of the perchlorate anion with the two Ag–N bonds equal to 2.208(2) Å and the two Ag–O bonds equal to 2.627(2) Å. The N1–Ag1–N1 bite angle of the silver complex is 140.56(7)°. With a

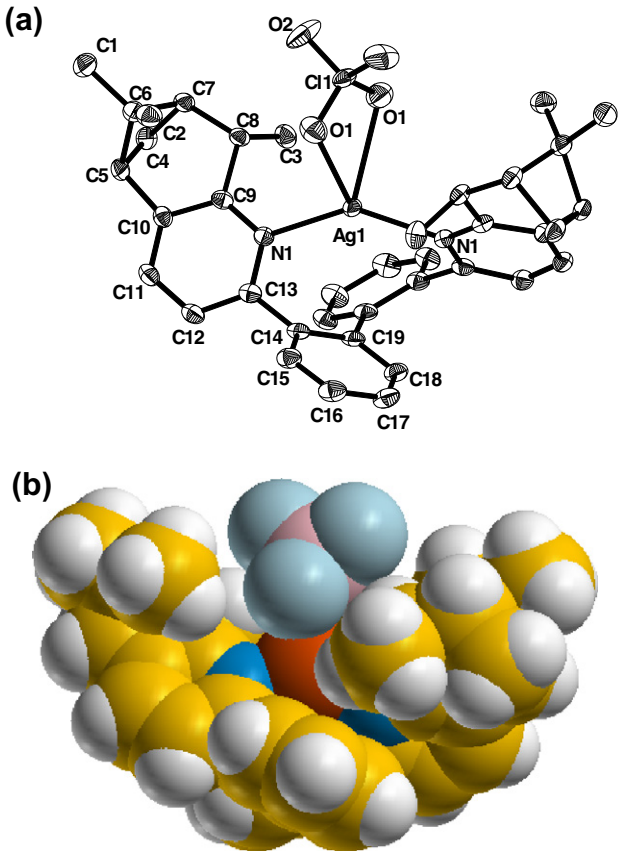

Fig. 5. (a) ORTEP plot of [Ag(**L2**)ClO_4]. The thermal ellipsoides are drawn at the 30% probability level. Hydrogen atoms have been omitted for clarity. (b) Space filling model of [Ag(**L2**)ClO_4]. The model was generated using data from the X-ray crystal structure.

2-fold symmetry, the two torsional angles between the pyridine and phenyl rings involving atoms N1–C13–C14–C19 are the same and equal to 53.8(3)°. The torsional angle between the phenyl rings involving atoms C14–C19–C19–C14 is 132.9(2)°. The sum of the torsional angles between the rings is equal to 240.61°. This twisting allows **L2** to act as a bidentate ligand.

On the other hand, the copper(I) center has a trigonal planar geometry, coordinating to the two pyridine nitrogen atoms of **L2** and one iodide (Fig. 6). With a 2-fold symmetry, the two Cu–N bond lengths are equal to 2.041(3) Å and the Cu–I bond equals 2.582(0) Å. The N1–Cu–N1 bite angle (130.7(1)°) is much larger than other common bidentate pyridyl ligands like bipyridine, pyridyl amine, dipyrdiyl-ketone, etc. The sum of the bond angles around the copper center, two N1–Cu–I (114.67(6)°) and N1–Cu–N1 (130.7(1)°), is equal to 360° which indicates that copper(I) is coplanar with the donor atoms. The two torsional angles between the pyridine and phenyl rings involving atoms N1–C7–C6–C1 are 49.2(4)° and the torsional angle between the phenyl rings involving atoms C6–C1–C1–C6 is 122.4(4)°. The sum of the torsional angles between the rings is now 200.74°. **L2** adopts a different degree of twisting in order to coordinate a metal with a different coordination geometry.

6. Coordination properties towards ammonium ions

Since pyridine is a common motif used in supramolecular chemistry for coordination with the ammonium ion via hydrogen bonding [32–37], the binding properties of the new biphenyl ligands towards amino acid derivatives were examined by NMR

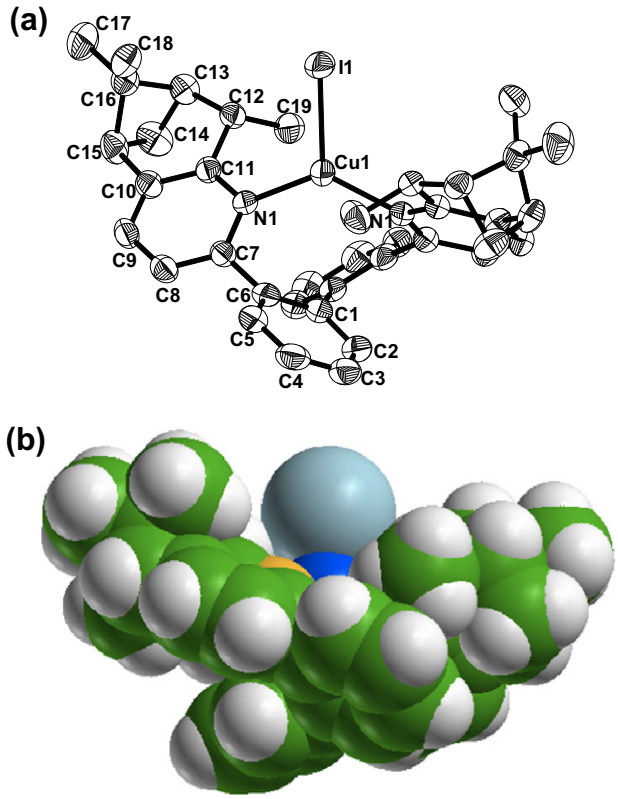

Fig. 6. (a) ORTEP plot of [Cu(**L2**)I]. The thermal ellipsoides are drawn at the 30% probability level. Hydrogen atoms have been omitted for clarity. (b) Space filling model of [Cu(**L2**)I]; The model was generated using data from the X-ray crystal structure.

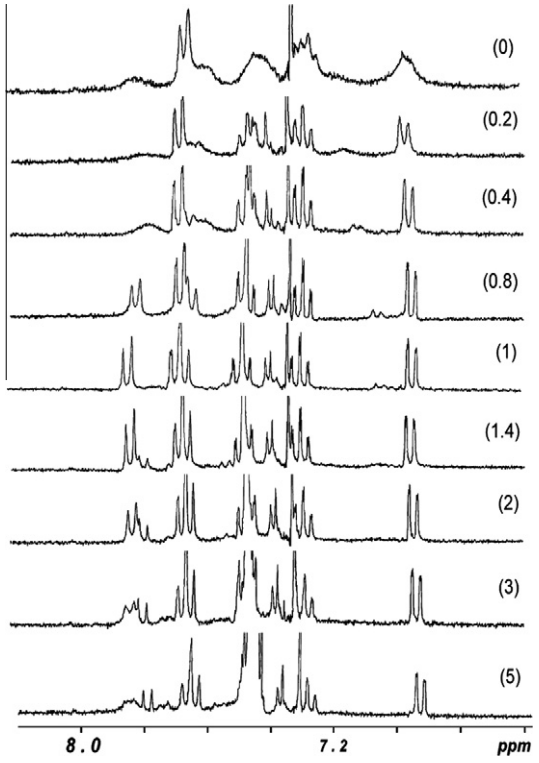

Fig. 7. ^{1}H NMR titration study of **L1** towards (*S*)-Ph-Gly in $CDCl_3$ with 5% CD_3OD, [**1**] = 5.0×10^{-3} M and [(*S*)-Ph-Gly] = 0 to 2.5×10^{-2} M. The numbers in parentheses indicate the number of equivalent of (*S*)-Ph-Gly added.

titration studies. Upon addition of (*S*)-phenylglycine methyl ester hydrochloride ((*S*)-Ph-Gly) to **L1** in $CDCl_3$ with 5% CD_3OD, the broad signals started to sharpen and only one set of proton signals was observed when one equivalent of (*S*)-Ph-Gly is present (Fig. 7). These results suggest the formation of a single diastereomeric 1:1 host–guest complex (**L1**·(*S*)-Ph-Gly), which is analogous to the silver and copper(I) complexes. Interestingly, when an excess of the ammonium guest was added, the two-proton doublet at 7.8 ppm became two one-proton doublets and broadening of other proton signals started to occur. These changes indicate that the unfixed biphenyl bridge may allow **L1** to bind to more than one ammonium ion and form a 1:2 host–guest complex.

To study the interesting binding properties of the biphenyl ligands towards ammonium ions, the photophysical properties of these biphenyl ligands were then investigated. In the fluorescent spectrum the biphenyl ligands exhibit a fluorescent emission peak at 372 nm in $CHCl_3$ with 5% CH_3OH. An excitation peak at a wavelength of 312 nm indicates a Stokes shift of 60 nm. Upon addition of (*R*)-Ph-Gly, the fluorescent emission peak corresponding to the ligand at 372 nm decreased gradually and a new peak started to appear at 430 nm upon addition of the guest (Fig. 8a). Interestingly, the emission peak shifted gradually from 430 to 400 nm with a high guest concentration, with a dramatic change in the fluorescence enhancement (about 5-fold more intense than the peak at 430 nm). Two major isosbestic points at 347 and 400 nm were observed in the titration curves. The shift in λ_{max} indicates a change in the twisting angle of the biphenyl bridge [21]. The results were then examined using the modified Hildebrand–Benesi equations [38]. The plot of $\boldsymbol{I_o}/(\boldsymbol{I}-\boldsymbol{I_o})$ versus $[\text{Ph-Gly}]^{-2}$ shows a very good linear relationship (R = 0.9998) with $\boldsymbol{K_{obs}}$ equal to 1.3×10^5 M^{-2} (the inset in Fig. 8), suggesting a 1:2 binding for Ph-Gly. The first

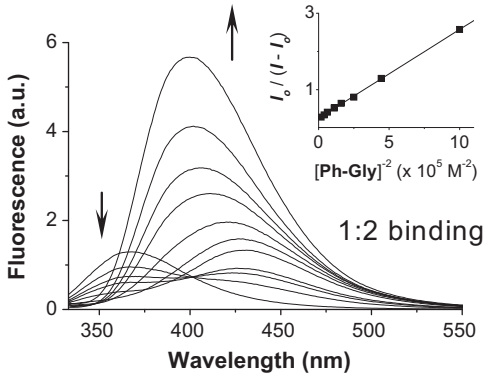

Fig. 8. Fluorimetric titration of **L1** (1.0×10^{-4} M in $CHCl_3$ with 5% CH_3OH, λ_{exc} = 323 nm, slit width = 4 nm) at 25 °C with (a) [Ph-Gly] = 0 to 7.5×10^{-3} M. The inserts showed the plot of $\boldsymbol{I_o}/(\boldsymbol{I}-\boldsymbol{I_o})$ versus $[\text{Ph-Gly}]^{-2}$ with [Ph-Gly]/[**L1**] = 1075 (R = 0.9998). a.u. = arbitrary unit.

equilibrium binding constant ($\boldsymbol{K_1}$) for Ph-Gly was also estimated at a low guest concentration [39].

The two pyridine rings of **L1** could bind to two ammonium ions, which make it a potential receptor for diammonium guests. Thus the binding between **L1** and L-ornithine methyl ester hydrochloride (Orn) was examined. Interestingly, a single isosbestic point at 400 nm with no shift in λ_{max} was observed (Fig. 9). On the contrary to the case for (*R*)-Ph-Gly, the Hildebrand–Benesi plot for Orn (the inset in Fig. 9) shows a 1:1 binding with $\boldsymbol{K}$ equal to 1.0×10^4 M^{-1} [40], which is about 4 times larger than the $\boldsymbol{K_1}$ value for Ph-Gly. These results indicate that the 1:1 host–guest complex of Orn is more stable than that of Ph-Gly. Moreover, the Job's plot analysis showed a 1:2 host–guest complex formation for Ph-Gly and a 1:1 complex formation for Orn.

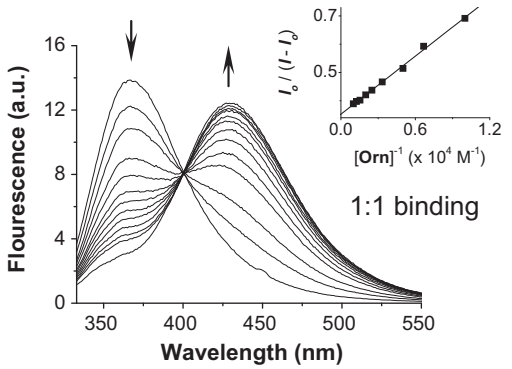

Fig. 9. Fluorimetric titration of **L1** (1.0×10^{-4} M in $CHCl_3$ with 5% CH_3OH, λ_{exc} = 323 nm, slit width = 4 nm) at 25 °C with [Orn] = 0 to 0.2×10^{-3} M. The insert showed the plot of $I_o/(I - I_o)$ versus $[Orn]^{-1}$ with [Orn]/[**L1**] = 0 to 10 (R = 0.9997).

The binding properties of **L1** towards a variety of amino esters were also studied. All the ammonium guests tested showed a shift in λ_{max}, such as L-serine methyl ester hydrochloride and L-phenylalanine methyl ester hydrochloride, as well as those bearing a cationic side-chain: L-lysine methyl ester hydrochloride (Lys) and L-arginine methyl ester hydrochloride (Arg). In spite of the structural similarity between Orn and Lys, **L1** exhibited a 1:2 binding towards Lys with K_{obs} equals 6.0×10^5 M^{-2}. This result indicates that **L1** is highly selective to the distance between the two chelating groups of the guest. A shift in λ_{max} was also observed upon addition of Arg. However, the K_{obs} value could not be determined due to a solubility problem of Arg in the high guest concentration. The enantioselectivity of **L1** towards some selected ammonium guests was also investigated and **L1** shows the highest enantioselectivity towards the (*R*)-enantiomer of Ph-Gly with $K_{obs}(R)/K_{obs}(S)$ equals 4.2 ($\Delta\Delta Go = -3.6$ kJ mol^{-1}) [41].

Since **L1** contains two potential binding sites (the two pyridine rings), two different binding mechanisms (a 1:2 stepwise binding for Ph-Gly and a 1:1 binding for Orn) are proposed (Fig. 10). The two pyridines of biphenyl **L1** would bind to one guest molecule with a "close" conformation in low guest concentration, forming a 1:1 host–guest complex. Thus both **L1** and **L2** would form the 1:1 host–guest complexes with similar twisting angles and lead to the same λ_{max} under the initial titration conditions. When the concentration of the guest increases, **L1** would bind to another molecule of Ph-Gly with an "open" conformation, in which the twisting angle of the biphenyl bridge is smaller than that of the "close" conformation, leading to a smaller λ_{max} for the 1:2 host–guest complex [21]. On the other hand, the 1:1 host–guest complex of Orn should be more stable than that of Ph-Gly due to the synergistic binding of the two pyridine rings with the two ammonium groups, and the formation of the 1:2 host–guest complex is not favorable even with a high guest concentration.

7. Conclusions

In summary, we have successfully developed the synthesis of new chiral dipyridine ligands containing an axially unfixed 1,1′-biphenyl bridge (**L1** and **L2**). The free biphenyl ligands show two rotational conformers in solution and NMR studies show that the conformeric ratios can be affected by hydrogen bonding between the ligands and the solvent molecules. In metal binding studies, **L2** forms a single diastereomeric complex with both silver(I) and copper(I) ions, but **L1** gives 4:1 and 2.9:1 diastereomeric ratios respectively. The X-ray crystal structures of [Ag(**L2**)ClO_4] and [Cu(**L2**)I] indicate that the major diastereomers should be the one with the *S* planar charity. In ammonium binding studies, the biphenyl ligand exhibits a 1:2 stepwise binding mechanism towards all the ammonium guests tested, with λ_{max} shifting from 430 to 400 nm and a strong fluorescence enhancement, but a selectively 1:1 binding is shown towards L-ornithine methyl ester hydrochloride with no shift in λ_{max}. The unique switching and binding properties of the biphenyl ligands towards amino acid derivatives and their distinct responses in fluorescence enhancement may lead to interesting applications in the design of switch-functionalized recognition systems.

8. Experimental section

8.1. General information

The solvents used for synthesis were of analytical grade. All starting chemicals were of reagent grade quality, obtained commercially and used without further purification. UV spectra were

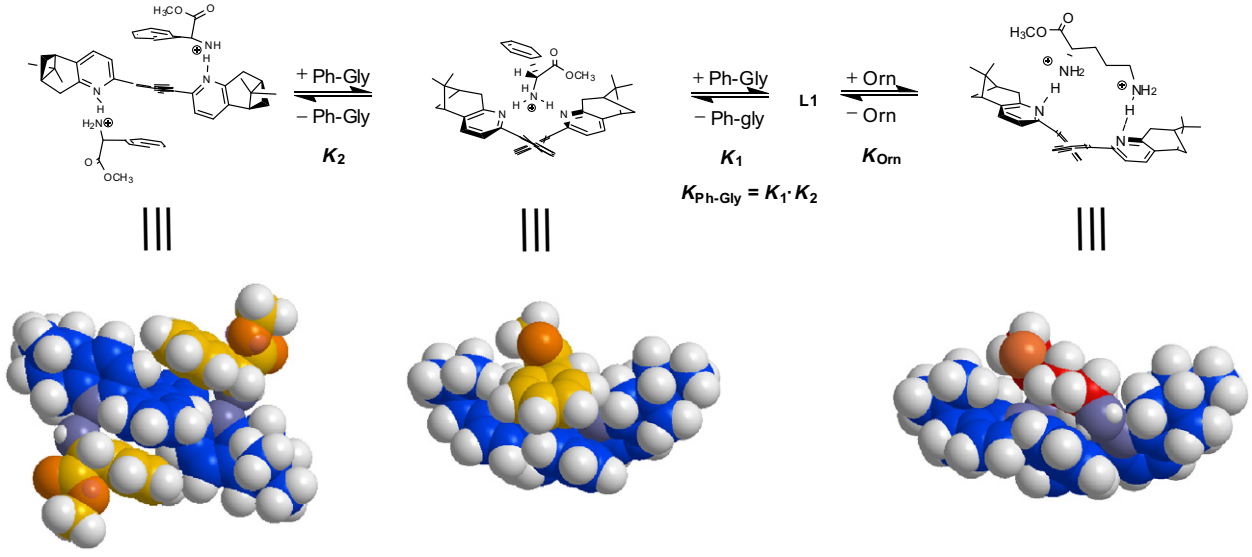

Fig. 10. A proposed mechanism for the binding of **L1** towards Ph-Gly (a 1:2 stepwise binding) and Orn (a 1:1 binding). The space filling models for the 1:1 and 1:2 host–guest complexes were generated using Chem3D.

recorded on a Hewlett–Packard 8452A ultraviolet visible diode array spectrophotometer. Electron ionization mass spectra were recorded on a Hewlett Packard 5890II GC instrument coupled with a 5970 mass selective detector. Elemental analyses were performed with a Vario EL elemental analyzer. Crystal data of [Cu(**L2**)I] and [Ag(**L2**)ClO_4] were collected at 301(2) and 133(2) K on a Bruker SMART 1000 CCD area detector with graphite monochromated Mo Kα and Cu Kα radiation, respectively (Table 2). All collected frames were processed with the software SAINT, and an absorption correction was applied (SAD-ABS) to the collected reflections. The structures of the complexes were solved by direct methods (SHELXTL) in conjunction with standard difference Fourier syntheses. All non-hydrogen atoms were assigned with anisotropic displacement parameters. The hydrogen atoms were generated in their idealized positions and allowed to ride on the respective carbon atoms.

8.2. Pyridinium iodide *1*

To a stirred solution of 2′-bromoacetophenone (1.0 g, 5.0 mmol) in pyridine (5 ml) was added iodine (2.54 g, 10 mmol). The resulting mixture was stirred at 100 °C for 3 h. The mixture was then cooled to 0 °C, and the precipitate was filtered and washed with ethanol to afforded a yellow solid (1.6 g, 4.0 mmol, 79%), which was used without further manipulation: IR (KBr, cm^{-1}): 3043 w, 1707 vs, 1632 s, 1470 s, 1168 s, 983 s, 765 vs, 690 s; ^{1}H NMR (300 MHz, $CDCl_3$) δ: 2.18 (s, 2H), 7.47 (t, J = 8 Hz, 1H), 7.57 (t, J = 7 Hz, 1H), 7.72 (dd, J = 7, 8 Hz, 1H), 8.15–8.21 (m, 3H), 8.58 (t, J = 7 Hz, 1H), 9.13 (m, 2H).

8.3. General procedure for bromophenyl pyridines *4*–*5*

To a stirred solution of pyridinium iodide **1** (1.5 mmol) and the appropriate ketone (**2**–**3**) (2.0 mmol) in glacial acetic acid (2 ml) was added ammonium acetate (2.0 g, 26 mmol). The resulting mixture was stirred at 120 °C for 16 h. The mixture was then neutralized using 2 N aqueous NaOH solution, and the aqueous layer was extracted with CH_2Cl_2 (10 ml × 3). The combined extracts were dried over $MgSO_4$, filtered and concentrated. The residue was purified by silica gel column chromatography (4% ethyl acetate in petroleum ether).

Table 2
Crystal data and structure refinement details for compounds [Ag(**L2**)ClO_4] and [Cu(**L2**)I]·CH_2Cl_2.

Compound	[Ag(**L2**)ClO_4]	[Cu(**L2**)I]·CH_2Cl_2
Formula	$C_{38}H_{40}N_2O_4ClAg$	$C_{39}H_{42}N_2Cl_2ICu$
Formula weight	732.04	800.09
Crystal system	Tetragonal	Tetragonal
Space group	P4(3)2(1)2	P4(3)2(1)2
Unit cell dimensions		
a (Å)	10.67225 (7)	10.3540(10)
b (Å)	10.67225 (7)	10.3540(10)
c (Å)	29.8044 (3)	33.639(3)
α (°)	90.00	90.00
β (°)	90.00	90.00
γ (°)	90.00	90.00
Cell volume (Å^3)	3394.62 (5)	3606.3(6)
Z	4	4
$D_{calc.}$ (g/cm^3)	1.432	1.474
μ (mm^{-1})	5.83	1.64
$F_{0\,0\,0}$	1512	1624
Temperature (K)	133(2)	296(2)
Radiation	Cu Kα	Mo Kα
λ (Å)	1.5418	0.7107
$\theta_{min,\ max}$ (°)	4.4, 71.6	2.1, 27.5
R_{int}	0.018	0.069
R_{all}, R_{obs}	0.0239, 0.0233	0.0530, 0.0337
wR_{all}, wR_{obs}	0.0588, 0.0585	0.0658, 0.0619
Flack	−0.012(6)	−0.028(19)
Measured reflections: total, unique	6443, 3247	21636, 4084
Goodness-of-fit on F^2	1.05	1.08

8.4. Bromophenyl pyridine *4*

The general procedure was followed with pyridinium iodide **1** (0.60 g, 1.5 mmol) and ketone **2** (0.30 g, 2.0 mmol). A yellowish brown oil (0.36 g, 0.89 mmol, 58%) was obtained: ^{1}H NMR (300 MHz, $CDCl_3$) δ: 0.70 (s, 3H), 1.34 (d, J = 10 Hz, 1H), 1.42 (s, 3H), 2.35−2.42 (m, 1H), 2.70 (td, J = 6, 10 Hz, 1H), 2.80 (t, J = 6 Hz, 1H), 3.18 (d, J = 3 Hz, 2H), 7.19 (dt, J = 2, 8 Hz, 1H), 7.25 (app s, 2H), 7.36 (td, J = 1, 8 Hz, 1H), 7.54 (dd, J = 2, 8 Hz, 1H), 7.64 (dd, J = 1, 8 Hz, 1H); ^{13}C NMR (300 MHz, $CDCl_3$) δ: 21.6, 26.3, 32.1, 36.9, 39.7, 40.5, 46.6, 121.3, 122.4, 127.6, 129.4, 131.7, 132.9, 133.4, 140.8, 141.9, 155.6, 156.7; Positive ion MS-ESI m/z: 328 (MH^+), 330 [$(M+2)H^+$].

8.5. Bromophenyl pyridine *5*

The general procedure was followed with pyridinium iodide **1** (0.60 g, 1.5 mmol) and ketone **3** (0.30 g, 2 mmol). A yellowish brown oil (0.26 g, 0.64 mmol, 42%) was obtained: ^{1}H NMR (300 MHz, $CDCl_3$) δ: 0.69 (s, 3H), 1.39 (d, J = 10 Hz, 1H), 1.44 (s, 3H), 1.44 (d, J = 7 Hz, 3H), 2.18 (dt, J = 2, 6 Hz, 1H), 2.58 (td, J = 5, 10 Hz, 1H), 2.81 (t, J = 6 Hz, 1H), 3.23−3.29 (m, 1H), 7.18−7.27 (m, 3H), 7.38 (dt, J = 2, 8 Hz, 1H), 7.57 (dd, J = 2, 8 Hz, 1H), 7.66 (dd, J = 1, 8 Hz, 1H); ^{13}C NMR (300 MHz, $CDCl_3$) δ: 18.5, 21.1, 26.6, 28.8, 39.1, 41.7, 47.1, 47.3, 121.3, 122.4, 127.6, 129.4, 131.8, 132.7, 133.6, 140.6, 141.9, 155.5, 160.6; Positive ion MS-ESI m/z: 342 (MH^+), 344 [$(M+2)H^+$].

8.6. General procedure for the biphenyl ligands *L1* and *L2*

To a stirred solution of bromophenyl pyridine **4** or **5** (0.5 mmol) in degassed DMF (5 ml) was added copper powder (10 mmol) under N_2. The resulting mixture was stirred under N_2 at 100 °C for 16 h. After removal of the copper powder by filtration, the solution was diluted with diethyl ether (30 ml) and extracted with 5% aqueous ammonia solution (5 ml × 3). The organic layer was dried over $MgSO_4$, filtered and concentrated. The residue was purified by silica gel column chromatography (5% ethyl acetate in petroleum ether).

8.6.1. *L1*

The general procedure was followed with bromophenyl pyridine **4** (0.16 g). An off-white solid (0.11 g, 0.22 mmol, 80%) was obtained: mp 122–123 °C; $[\alpha]_D^{25} = -125°$ (c 0.5, $CHCl_3$); ^{1}H NMR (300 MHz, $CDCl_3$, a mixture of biphenyl conformers) δ: 0.46 (bs, 3H), 0.62 (s, 3H), 1.12–1.23 (m, 2H), 1.29 (d, J = 10 Hz, 2H), 1.37 (s, 6H), 2.262.32 (m, 2H), 2.60–2.79 (m, 4H), 2.79–3.02 (m, 4H), 6.64 (bs, 1H), 6.94 (m, 1H), 7.02 (d, J = 8 Hz, 2H), 7.157.29 (m, 4H), 7.35 (app t, J = 8 Hz, 2H), 7.60 (d, J = 8 Hz, 1H), 7.68 (d, J = 8 Hz, 1H); ^{13}C NMR (300 MHz, $CDCl_3$, a mixture of biphenyl conformers) δ: 15.9, 16.1, 20.9, 26.7, 26.9, 30.5, 31.0, 34.3, 34.9, 41.0, 55.3, 116.1, 116.6, 122.1, 122.6, 124.2, 124.5, 125.9, 126.2, 127.7, 134.3, 135.3, 135.5, 149.8, 150.2; Anal. Calc. for $C_{36}H_{36}N_2·0.5H_2O$: C, 85.50; H, 7.37; N, 5.54; Found: C, 84.88; H, 7.32; N 5.53; Positive ion MS-ESI m/z: 497 (MH^+).

8.6.2. *L2*

The general procedure was followed with bromophenyl pyridine **5** (0.17 g). An off-white solid (0.07 g, 0.13 mmol, 46%) was obtained: ^{1}H NMR (400 MHz, $CDCl_3$, a mixture of biphenyl conformers) δ: 0.54 (s, 6H), 0.66 (s, 6H), 0.75 (d, J = 7.2 Hz, 6H),

1.30 (d, J = 7.2 Hz, 6H), 1.36 (s, 6H), 1.40 (s, 6H), 2.03 (m, 2H), 2.08 (m, 2H), 2.5 (m, 4H), 2.62 (t, J = 6 Hz, 2H), 2.69 (m, J = 6 Hz, 2H), 2.84 (m, 2H), 3.14 (m, 2H), 6.22 (d, J = 7.6 Hz, 2H), 6.76 (d, J = 5.2 Hz, 2H), 6.78 (d, J = 4.8 Hz, 2H), 7.20 (m, 4H), 7.17 (d, J = 8.0 Hz, 2H), 7.28 (m, 6H), 7.43 (t, J = 6 Hz, 2H), 7.57 (d, J = 7.2 Hz, 2H), 7.70 (d, J = 6.8 Hz, 2H); ^{13}C NMR (300 MHz, $CDCl_3$, a mixture of biphenyl conformers) δ: 10.0, 10.1, 19.2, 20.0, 20.1, 26.2, 26.3, 30.4, 31.4, 31.5, 51.3, 51.4, 53.8, 56.5, 56.6, 76.6, 120.7, 126.4, 126.6, 127.1, 127.2, 127.3, 127.5, 129.2, 129.4, 131.5, 138.2, 140.3, 140.5, 141.6, 141.9, 155.0, 155.2, 168.9; Anal. Calc. for $C_{38}H_{40}N_2{\cdot}2H_2O$: C, 81.39; H, 7.91; N, 5.00; Found: C, 81.11; H, 7.71; N 5.23; Positive ion MS-ESI m/z: 525 (MH^+).

8.6.3. Caution

Perchlorate salts are potentially explosive and should be treated with extra care. Those complexes described below which were isolated as perchlorates were only prepared in small amounts which did not cause any problem in handling.

*8.7. General procedure for [Ag(L)ClO_4] (**L** = **L1** and **L2**)*

Methanol (2 ml) was added to a flask containing **L** (0.12 mmol) and $AgClO_4$ (0.12 mmol) that was covered with foil. The mixture was stirred for 12 h. The white precipitated product was collected by filtration and washed with diethyl ether (10 ml × 3).

*8.7.1. [Ag(**L1**)ClO_4]*

The general procedure was followed with **L1** (0.060 g). A white solid (0.053 g, 0.076 mmol, 64%) was obtained: Anal. Calc. for $C_{36}H_{36}N_2AgClO_4$: C, 61.4; H, 5.15; N, 3.98. Found: C, 61.2; H, 5.15; N, 4.08. Positive ion MS-ESI m/z: 603 $(M-ClO_4)^+$.

*8.7.2. [Ag(**L2**)ClO_4]*

The general procedure was followed with **L2** (0.063 g). A white solid (0.066 g, 0.09 mmol, 75%) was obtained: Anal. Calc. for $C_{38}H_{40}N_2AgClO_4{\cdot}1/4CH_2Cl_2$: C, 61.0; H, 5.42; N, 3.72. Found: C, 61.1; H, 5.43; N, 3.81. Positive ion MS-ESI m/z: 631 $(M-ClO_4)^+$.

*8.8. General procedure for [Cu(L)I] (**L** = **L1** and **L2**)*

Degassed MeCN (6 ml) was added to a flask containing **L** (0.12 mmol) and CuI (0.12 mmol) under nitrogen. The mixture was stirred for 12 h. It was reduced to minimum amount of solvent. Dichloromethane (2 ml) was added, then n-hexane (40 ml) was added to precipitate out the product. The product was collected by filtration and washed with n-hexane (20 ml × 3).

*8.8.1. [Cu(**L1**)I]*

The general procedure was followed with **L1** (0.061 g). A yellow solid (0.050 g, 0.072 mmol, 60%) was obtained: Anal. Calc. for $C_{36}H_{36}N_2CuI$: C, 62.9; H, 5.28; N, 4.08. Found: C, 62.7; H, 5.11; N, 3.92. Positive MS-ESI m/z: 559 $(M-I)^+$.

*8.8.2. [Cu(**L2**)I]*

The general procedure was followed with **L2** (0.063 g). A yellow solid (0.055 g, 0.076 mmol, 63%) was obtained: Anal. Calc. for $C_{34}H_{40}N_2CuI{\cdot}1/5CH_2Cl_2$: C, 62.7; H, 5.56; N, 3.82. Found: C, 62.8; H, 5.59; N, 3.82. Positive MS-ESI m/z: 587 $(M-I)^+$.

Acknowledgment

The work described in this paper was supported by a grant from the University Grants Committee of the Hong Kong Special Administrative Region, China (Project No. [AoE/P-03/08]) and the City University of Hong Kong (Project No.7002607).

Appendix A. Supplementary data

CCDC 796015 and 796016 contain the supplementary crystallographic data for [Ag(**L2**)(ClO_4)] and [Cu(**L2**)I] respectively. These data can be obtained free of charge via http://www.ccdc.cam.ac.uk/conts/retrieving.html, or from the Cambridge Crystallographic Data Centre, 12 Union Road, Cambridge CB2 1EZ, UK; fax: (+44) 1223-336-033; or e-mail: deposit@ccdc.cam.ac.uk.

References

[1] J. Reedijk, G. Wilkinson (Eds.), Comprehensive Coordination Chemistry, vol. 2, Pergamon Press, London, 1987. 73.
[2] A.G. Blackman, Eur. J. Inorg. Chem. (2008) 2633–2647.
[3] H.-L. Kwong, H.-L. Yeung, C.-T. Yeung, W.-S. Lee, C.-S. Lee, W.-L. Wong, Coor. Chem. Rev. 251 (2007) 2188.
[4] O. Mamula, A. Von Zelewsky, Coor. Chem. Rev 242 (2003) 87.
[5] M.D. Ward, J.A. McCleverty, J.C. Jeffery, Coor. Chem. Rev. 222 (2001) 251.
[6] T.C. Stamatos, C.G. Efthymiou, C.C. Stoumpos, S.P. Perlepes, Eur. J. Inorg. Chem. (2009) 3361.
[7] C. Kaes, A. Katz, M.W. Hosseini, Chem. Rev 100 (2000) 3553.
[8] M. Ruben, J. Rojo, R. Salguero, L.H. Uppadine, J.-M. Lehn, Angew. Chem., Int. Ed. 43 (2004) 3644.
[9] Y. Guo, W. Dou, X. Zhou, W. Liu, W. Qln, Z. Zang, H. Zhang, D. Wang, Inorg. Chem. 48 (2009) 3581.
[10] L.T. Dulatas, S.N. Brown, E. Ojomo, B.C. Noll, M.J. Cavo, P.B. Holt, M.M. Wopperer, Inorg. Chem. 48 (2009) 10789.
[11] C. Vedder, F. Schaper, H.-H. Brintzinger, M. Kettunen, S. Babik, G. Fink, Eur. J. Inorg. Chem. (2005) 1071.
[12] D.P. Goldberg, A. Caneschi, S.J. Lippard, J. Am. Chem. Soc. 115 (1993) 9299.
[13] S.-Q. Zang, L. Zhao, T.C.W. Mak, Organometallics 27 (2008) 2396.
[14] D. Cunningham, K. Gilligan, M. Hannon, C. Kelly, P. McArdle, A. O'Malley, Organometallics 23 (2004) 984.
[15] C. Mukherjee, T. Weyhermüller, E. Bothe, P. Chaudhuri, Inorg. Chem. 47 (2008) 11620.
[16] E. Müller, C. Piguet, G. Bernardinelli, A.F. Williams, Inorg. Chem. 27 (1988) 849.
[17] J. Chen, R. Russo, W. Chao, L.D. Margerum, M.R. Malachowski, R. White, Z. Thawley, A. Thayer, A.L. Rheingold, L.N. Zakharov, J. Chem. Soc., Dalton Trans. (2007) 2571.
[18] P. Hormnirun, E.L. Marshall, V.C. Gibson, R.I. Pugh, A.J.P. White, Proc. Natl. Acad. Sci. USA 103 (2006) 15343.
[19] Y.J. Zhang, F. Wang, W. Zhang, J. Org. Chem. 72 (2007) 9208.
[20] P.S. Singh, H.C. Rubeck, P. Huang, S. Ezzaher, L. Eriksson, M. Stein, S. Ott, R. Lomoth, Inorg. Chem. 48 (2009) 10883.
[21] M. Maus, W. Rettig, J. Phys. Chem. A 106 (2002) 2104.
[22] Z.-H. Lin, L.-X. Xie, Y.-G. Zhao, C.-Y. Duan, J.-P. Qu, Org. Biomol. Chem. 5 (2007) 3535.
[23] D.-Y. Wu, L.-X. Xie, C.-L. Zhang, C.-Y. Duan, Y.-G. Zhao, Z.-J. Guo, J. Chem. Soc., Dalton Trans. (2006) 3528.
[24] J. Cody, C.J. Fahrni, Tetrahedron 60 (2004) 11099.
[25] D.H. Lee, J.H. Im, J.-H. Lee, J.-I. Hong, Tetrahedron Lett. 43 (2002) 9637.
[26] T. Mizuno, M. Yamamoto, M. Takeuchi, S. Shinkai, Tetrahedron 56 (2000) 6193.
[27] A.M. Costero, J. Sanchis, S. Gil, V. Sanz, J.A. Gareth Williams, J. Mater. Chem. 15 (2005) 2848.
[28] M. Teng, G. Kuang, X. Jia, M. Gao, Y. Li, Y. Wei, J. Mater. Chem. 19 (2009) 5648.
[29] H.-L. Kwong, L.-S. Cheng, W.-S. Lee, W.-L. Wong, W.-T. Wong, Eur. J. Inorg. Chem. (2000) 1997.
[30] M. Düggeli, C. Goujon-Ginglinger, S.R. Ducotterd, D. Mauron, C. Bonte, A. von Zelewsky, H. Steockli-Evans, A. Neels, Org. Biomol. Chem. (2003) 1894.
[31] J.W. Akitt, B.E. Mann, NMR and Chemistry: An introduction to modern NMR spectroscopy, Stanley Thornes Ltd., Cheltenham, 2000.
[32] C.R.K. Glasson, L.F. Lindoy, G.V. Meehan, Coord. Chem. Rev 252 (2008) 940.
[33] T. Sugimoto, T. Suzuki, S. Shinkai, K. Sada, J. Am. Chem. Soc. 129 (2007) 270.
[34] C.-S. Lee, P.-F. Teng, W.-L. Wong, H.-L. Kwong, A.S.C. Chan, Tetrahedron 61 (2005) 7924.
[35] W.-L. Wong, K.-H. Huang, P.-F. Teng, C.-S. Lee, H.-L. Kwong, Chem. Commun. (2004) 384.
[36] T.W. Bell, A.B. Khasanov, M.G.B. Drew, J. Am. Chem. Soc. 124 (2002) 14092.
[37] T. Chang, A.M. Heiss, S.J. Cantrill, M.C.T. Fyfe, A.R. Pease, S.J. Rowan, J.F. Stoddart, A.J.P. White, D.J. Williams, Org. Lett. 2 (2000) 2947.
[38] Binding constants: the measurement of molecular complex stability; Wiley: New York, 1987.

$$I_o/(I-I_o) = (a/(b-a))(1/K[G]^{-1}+1) \quad (1)$$

$$I_o/(I-I_o) = (c/(d-c))(1/K[G]^{-2}+1) \quad (2)$$

where a, b, c and d are constants.

[39] Determination of K_1 for Ph-Gly: [**1**] = 1.0×10^{-4} M in $CHCl_3$ with 5% CH_3OH at 25 °C, and [Ph-Gly] = 0 to 1.0×10^{-4} M ([Ph-Gly]/[**1**] = 0 to 1). The fluorescence emission intensity was observed at 430 nm (λ_{exc} = 323 nm, slit width = 4 nm). By using Eq. 1, K_1 was estimated to be 2.4×10^3 M^{-1} with R = 0.9998. Thus K_2 equals 54 M^{-1}.

[40] Determination of K for Orn: [**1**] = 1.0×10^{-4} M in $CHCl_3$ with 5% CH_3OH at 25 °C, and [Orn] = 0 to 2.0×10^{-3} M ([Orn]/[**1**] = 0 to 10). The fluorescence emission intensity was observed at 430 nm (λ_{exc} = 323 nm and slit width = 4 nm), and the binding constants were estimated using Eq. 1.

[41] **L1** showed virtually no enantioselectivity towards Orn. This may be due to the non-selective binding of its achiral side-chain in the 1:1 binding mode.